Biochemistry

Article

Cite This: Biochemistry 2018, 57, 614−619

pubs.acs.org/biochemistry

Reshaping the Energy Landscape Transforms the Mechanism and Binding Kinetics of DNA Threading Intercalation

Andrew G. Clark,[†] M. Nabuan Naufer,[†] Fredrik Westerlund,[‡] Per Lincoln,[§] Ioulia Rouzina,[∥] Thayaparan Paramanathan,*[,⊥] and Mark C. Williams*[,†]

[†]Department of Physics, Northeastern University, Boston, Massachusetts 02115, United States

[‡]Department of Biology and Biological Engineering, Chalmers University of Technology, SE-412 96 Gothenburg, Sweden

[§]Department of Chemistry and Chemical Engineering, Chalmers University of Technology, SE-412 96 Gothenburg, Sweden

[∥]Department of Chemistry and Biochemistry, The Ohio State University, Columbus, Ohio 43210, United States

[⊥]Department of Physics, Bridgewater State University, Bridgewater, Massachusetts 02325, United States

Supporting Information

ABSTRACT: Molecules that bind DNA via threading intercalation show high binding affinity as well as slow dissociation kinetics, properties ideal for the development of anticancer drugs. To this end, it is critical to identify the specific molecular characteristics of threading intercalators that result in optimal DNA interactions. Using single-molecule techniques, we quantify the binding of a small metal−organic ruthenium threading intercalator (Δ,Δ-**B**) and compare its binding characteristics to a similar molecule with significantly larger threading moieties (Δ,Δ-**P**). The binding affinities of the two molecules are the same, while comparison of the binding kinetics reveals significantly faster kinetics for Δ,Δ-**B**. However, the kinetics is still much slower than that observed for conventional intercalators. Comparison of the two threading intercalators shows that the binding affinity is modulated independently by the intercalating section and the binding kinetics is modulated by the threading moiety. In order to thread DNA, Δ,Δ-**P** requires a "lock mechanism", in which a large length increase of the DNA duplex is required for both association and dissociation. In contrast, measurements of the force-dependent binding kinetics show that Δ,Δ-**B** requires a large DNA length increase for association but no length increase for dissociation from DNA. This contrasts strongly with conventional intercalators, for which almost no DNA length change is required for association but a large DNA length change must occur for dissociation. This result illustrates the fundamentally different mechanism of threading intercalation compared with conventional intercalation and will pave the way for the rational design of therapeutic drugs based on DNA threading intercalation.

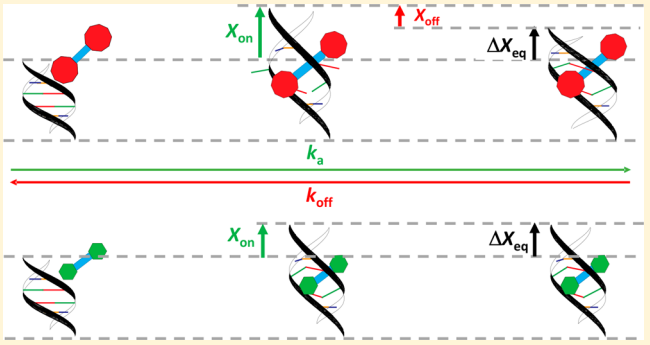

Developing new anticancer therapies that target DNA requires molecules that display high binding affinity to DNA as well as slow dissociation kinetics from DNA.[1−3] Anticancer drugs that target DNA have been shown to covalently cross-link DNA,[4] non-covalently bind to specific sequences or grooves,[5−7] or bind non-covalently via intercalation and base-stacking interactions.[8] In light of this observation, several ruthenium-based complexes have been synthesized that demonstrated effective mutagenic[9] and anticancer properties,[10,11] and a few have even entered clinical trials.[12−14] Polypyridyl ruthenium complexes with high binding affinities, first synthesized in the 1980s, were shown to bind to DNA via intercalation.[15] These metal−organic ruthenium complexes were later modified by covalently linking two ligands in order to further increase the DNA binding affinity.[16] This resulted in a group of new ruthenium-based compounds (examples are shown in Figure 1A,B) that bind to DNA via a modified form of intercalation known as threading, which involves forcing a bulky ruthenium center through double-stranded DNA (dsDNA).[17−19] Threading intercalators display even higher binding affinity, with dissociation constants in the nanomolar range, as well as particularly slow dissociation kinetics, with unbinding occurring on the order of hours to days.[20,21] It is the large positive charge, the strong stacking of aromatic groups with the DNA bases, and the favorable interaction of the ligand ancillary groups with the intercalated duplex that lead to such high affinity. The strong DNA deformation required for both binding and unbinding of such threading intercalators leads to their slow dissociation.[21] There is great potential for molecules that bind to DNA via threading to serve as anticancer drugs, with some current anticancer drugs such as nogalamycin having been identified as threading

Received: October 12, 2017
Revised: December 14, 2017
Published: December 15, 2017

DOI: 10.1021/acs.biochem.7b01036
Biochemistry 2018, 57, 614−619

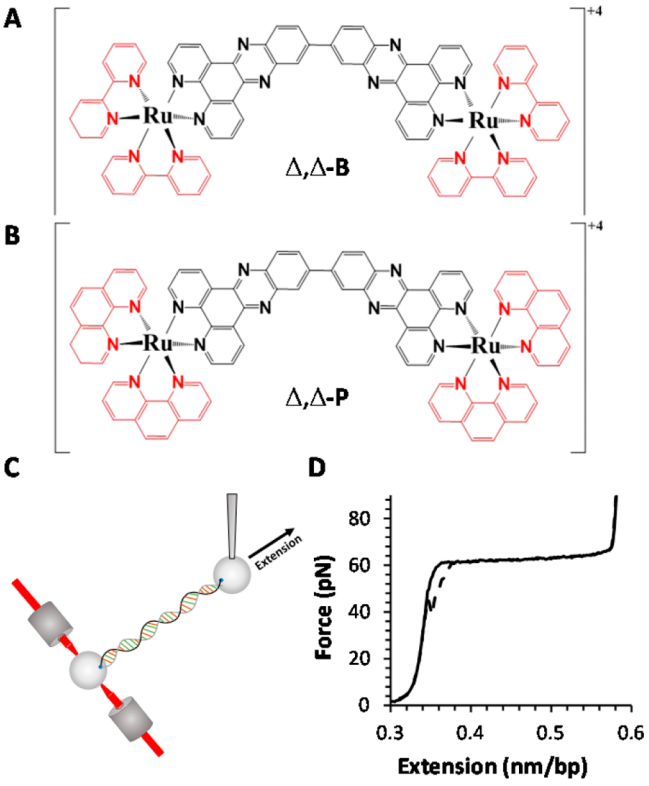

Figure 1. (A) Structure of Δ,Δ-$[\mu$-bidppz$(bpy)_4Ru_2]^{4+}$ and (B) Δ,Δ-$[\mu$-bidppz$(phen)_4Ru_2]^{4+}$ with ancillary motifs (shown in red) showcasing the difference in steric bulk. (C) Schematic of the optical tweezers instrument. (D) Canonical DNA stretch (solid) and release (broken) curve as measured using optical tweezers.

intercalators.[22] Identifying the specific molecular characteristics that affect DNA threading intercalation is of critical importance, as it allows for improved rational drug design.[23] Polypyridyl ruthenium complexes are ideally suited for studying the impact of molecular characteristics on DNA threading intercalation because of the ability to create molecules that differ from each other by only one characteristic, such as chirality, steric bulk, or planar surface area. Many polypyridyl ruthenium threading intercalators of the form $[\mu\text{-B(L)}_4\text{Ru}_2]^{4+}$ (where B is a tetradentate bridging ligand comprising two 1,10-phenanthroline units and L is an ancillary bidentate ligand) have been synthesized,[24−26] and their binding to DNA has been investigated through bulk luminescence and dichroism experiments.[26] Despite the striking structural similarities between these molecules, they all display significantly different binding kinetics and affinities. A recent single-molecule study revealed and quantified the profound effect that the chirality of the threading moiety has on the affinity and kinetics of threading intercalation.[27] In light of this work, we here seek to isolate and quantify the effect that the steric bulk of the threading moiety has on the binding of this class of threading intercalators to DNA.

The ligand of interest in this study is the semirigid ΔΔ-$[\mu$-bidppz$(bpy)_4Ru_2]^{4+}$ (Δ,Δ-**B**) (Figure 1A), which we seek to compare to the prototypical binuclear ruthenium threading intercalator ΔΔ-$[\mu$-bidppz$(phen)_4Ru_2]^{4+}$ (Δ,Δ-**P**) (Figure 1B). These two molecules are identical except for the sterically smaller bipyridine ancillary motifs attached to the ruthenium center in Δ,Δ-**B** compared with the larger phenanthroline motifs of Δ,Δ-**P**. Previous studies have shown that the dipyridophenazine (dppz) motifs show higher affinity for intercalating DNA compared with phenanthroline or bipyridine motifs for monomeric complexes.[28,29] This suggests that the central dppz sections of these molecules have higher affinity to intercalate, which has been structurally observed in the final binding configuration to DNA.[26] Previous studies have shown that small changes in these ligands may have significant effects on their DNA interactions.[21] However, because the direct DNA binding interactions occur in the center of both of these molecules, we hypothesized that changing only the ancillary motifs would isolate the threading process itself from the final equilibrium state.

MATERIALS AND METHODS

All of the experiments were conducted using a dual-beam optical tweezers setup.[30] Two counterpropagating diode lasers with λ = 830 nm were used to create an optical trap inside a custom-made flow cell. A micropipette with a tip diameter of 1 μm was affixed inside the cell to hold a 5.6 μm streptavidin-coated polystyrene bead using suction, while the optical trap held another identical bead. The flow cell was held by a piezoelectric stage that allowed for precise manipulations of the micropipette tip. λ-phage DNA (contour length of 48 502 bp) labeled with biotin at the 3′-end on opposite strands was flowed into the cell until a molecule was attached between the two beads. The cell was subsequently washed out with buffer, allowing for manipulation and measurement of the single DNA molecule caught between the two beads. Prior to introducing Δ,Δ-**B** into the cell, the DNA was stretched and returned in order to confirm that only a single molecule was trapped between the beads. Once properly characterized, the DNA was quickly stretched to the desired force and held at that constant tension via a feedback loop. The ligand was then introduced into the cell at a constant flow rate, allowing it to bind to the stretched DNA. The feedback loop was continued until the DNA−ligand binding reached equilibrium while maintaining a constant flow rate, after which the DNA was returned and discarded. All of the experiments were conducted in 10 mM Tris buffer with 100 mM Na^+ with a pH of 8 at 21 °C. The Δ,Δ-**B** ligands were synthesized as described elsewhere.[31] Data analysis methods are described in the Supporting Information.

RESULTS

We probed binding of Δ,Δ-**B** to DNA using single-molecule force spectroscopy with a dual-beam optical tweezers setup (Figure 1C), where the DNA can be stretched and characterized (Figure 1D).[3] Intercalation into DNA can be facilitated by force,[32] which provides a convenient means to quantify the ultraslow binding of Δ,Δ-**B** to DNA. The DNA is rapidly stretched to the desired force, and a feedback loop keeps the DNA under tension at that desired force. A specific concentration of ligand is then supplied to the DNA and subsequently binds to it, causing extension of the DNA, which is a characteristic of intercalation. The DNA is held at constant force long enough to reach an equilibrium extension and then is returned to zero force. The extension is measured as a function of time at various forces and concentrations of ligand (Figure 2A), which allows for both equilibrium and kinetic characterization of the binding (see the Supporting Information).[27,30] Characterization of binding at various forces allows for extrapolation to the zero-force binding limit.[28]

DOI: 10.1021/acs.biochem.7b01036
Biochemistry 2018, 57, 614−619

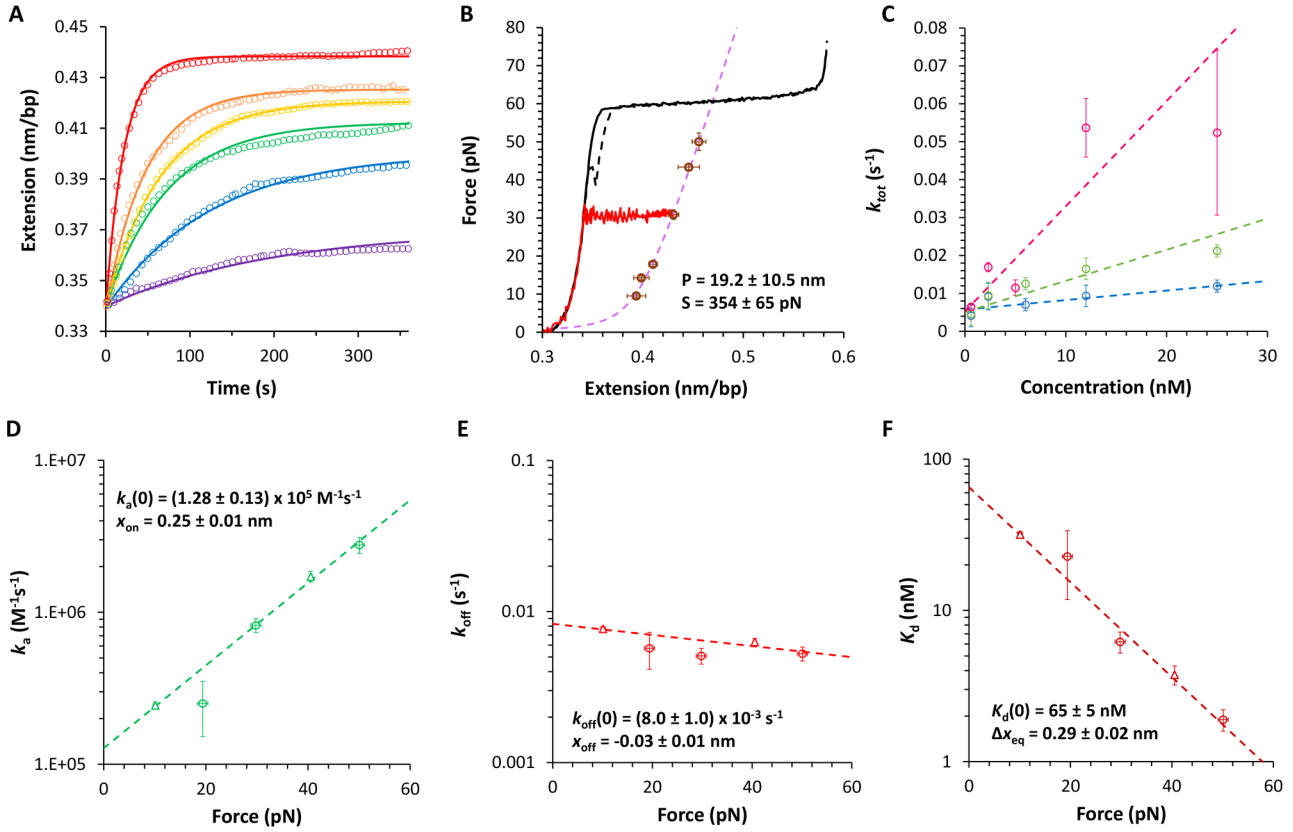

Figure 2. Constant-force measurements and analysis. (A) DNA extensions (open circles) in the presence of 0.6 (violet), 2.3 (blue), 6.0 (green), 12 (yellow), 25 (orange), and 90 (red) nM Δ,Δ-**B** as functions of time at a constant force of 29.8 ± 0.3 pN. Single-exponential fits are shown as solid lines. (B) Extension of DNA while rapidly stretching to 29.8 ± 0.3 pN and holding at constant force in the presence of saturated concentration of Δ,Δ-**B** (solid red line). Saturated extensions obtained at various forces (dark red circles) were fit to the wormlike chain polymer model (dashed lilac line) to obtain the effective elastic properties of the saturated DNA/ligand complex (parameters as shown). (C) Net relaxation rates k_{tot} obtained from the exponential fits in (A) (open circles) as functions of concentration with linear fits (dashed lines) at forces of 50.1 ± 0.3 pN (pink), 29.8 ± 0.3 pN (green), and 19.4 ± 0.7 pN (blue). (D) Association rates k_a obtained from the linear fits in (C) (circles) exhibiting exponential facilitation by force (dashed line), yielding the structural change and zero-force association rate (parameters as shown). (E) Off rates k_{off} obtained from the linear fits in (C) (circles) fitted to an exponential dependence on force (dashed line), yielding the structural changes required to unbind the drug (parameters as shown) and showing no facilitation by force. (F) Dissociation constants K_d estimated from the data in (D) and (E) (circles), exhibiting an exponential dependence on force (dashed line) and yielding the equilibrium binding parameters (as shown). Triangle symbols in (D–F) were obtained using an alternative kinetics method that directly measures k_{off}, as described in the Supporting Information.

The kinetics of binding of Δ,Δ-**B** to DNA fit well to a single-exponential dependence (Figure 2A), which indicates a one-step binding event on the time scales accessible to these experiments, which is characteristic of threading intercalation.[21] At each force, the saturated DNA extension was measured, and the data were fit to the modified wormlike chain (WLC) model in order to quantify the effective elastic properties of the saturated Δ,Δ-**B**/DNA complex (Figure 2B). The persistence length of the complex was measured to be 19.2 ± 10.5 nm, which is 3 times more flexible than dsDNA but an order of magnitude stiffer than the saturated Δ,Δ-**P**/DNA complex.[30] The stretch modulus of the Δ,Δ-**B**/DNA complex was measured to be 354 ± 65 pN, which is again significantly smaller than the stretch modulus of dsDNA and also smaller than the stretch modulus of the Δ,Δ-**P**/DNA complex.[21] Interestingly, the effective elastic properties of the Δ,Δ-**B**/DNA complex are strikingly similar to the properties measured for the monomeric Δ-**P**/DNA complex (Table S1 in the Supporting Information).[28] These properties are an indication of the level of deformation of the DNA duplex when bound by the ligand. Thus, they provide insight into the effect that steric bulk has on threading-induced DNA deformation. The sterically smaller Δ,Δ-**B** deforms the DNA far less than its parent molecule Δ,Δ-**P**, and the deformation is closer to that induced by monomeric Δ-**P**, which intercalates DNA without threading. Crystal structures for Δ,Δ-**P**, Δ-**B**, and Λ-**P** all indicate that one of the ruthenium centers sits in the DNA minor groove, which results in the distortion of the duplex.[33−35] These effective elastic properties indicate that the smaller Δ,Δ-**B** sits more compactly in the minor groove, resulting in less duplex deformation when bound in comparison with Δ,Δ-**P**.

Characterization of the binding kinetics was performed using the total relaxation rate, k_{tot} (Supporting Information eq 1). Figure 2A presents sample data obtained at 29.8 pN and increasing concentrations of Δ,Δ-**B**. At each force, the relaxation rate was plotted as a function of concentration and fit to a linear function (Figure 2C). Each linear fit returned the force-dependent association rate k_a and the off rate k_{off} (Supporting Information eq 3). The association and off rates were then plotted as functions of the force (open circles in Figure 2D,E, respectively) and also used to determine the force-dependent dissociation constant K_d (Supporting Information eq 5). The dissociation constants were also plotted as a function of force (open circles in Figure 2F). All three binding

DOI: 10.1021/acs.biochem.7b01036
Biochemistry 2018, 57, 614−619

parameters (k_a, k_{off}, and K_d) were fit to an exponential force dependence (dashed lines in Figure 2D−F) in order to extrapolate to the zero-force binding limit (Supporting Information eqs 4 and 6). Data points at 10 and 40 pN in Figure 2D−F were also obtained by measuring k_{off} directly (Figure S1 in the Supporting Information).

DISCUSSION

The returned zero-force association rate obtained from the combination of the kinetics analysis shown above (Figure 2) and the equilibrium extension analysis discussed in the Supporting Information, $k_a(0) = (1.21 \pm 0.12) \times 10^5$ M^{-1} s^{-1}, is approximately 1 order of magnitude larger than the value reported for Δ,Δ-**P**.[30] The zero-force off rate for Δ,Δ-**B** was measured to be $k_{off}(0) = (7.1 \pm 0.6) \times 10^{-3}$ s^{-1}, which is approximately 4 times the value reported for Δ,Δ-**P**.[30] These values are in agreement with the full association and dissociation times of the two ligands reported in the bulk studies.[20,36] The variation in kinetics indicates the modulating effect that steric bulk has on the rate of threading into dsDNA. Interestingly, although higher-affinity threading ligands have been reported,[37] the zero-force dissociation constants for these ligands are very similar (65 ± 5 nM for Δ,Δ-**B** and 44 ± 2 nM for Δ,Δ-**P**).

The binding affinity shows little dependence on the steric bulk of the threading subunit, which suggests that the steric bulk affects only the kinetics of binding. These measurements also reveal the DNA deformation associated with the DNA binding of Δ,Δ-**B**. The exponential force dependences return values for the DNA elongation required for the association of one ligand (x_{on}) and the elongation required for the dissociation of one ligand (x_{off}). From these two values, the equilibrium elongation of the DNA can be defined as $\Delta x_{eq} = x_{on} - x_{off}$. For Δ,Δ-**B**, the values obtained by combining the kinetics analysis shown in Figure 2 and the equilibrium analysis shown in the Supporting Information are $x_{on} = 0.26 \pm 0.01$ nm and $x_{off} = -0.02 \pm 0.01$ nm, which give $\Delta x_{eq} = 0.28 \pm 0.02$ nm. This calculated value for Δx_{eq} agrees within error with the value returned from fitting K_d as a function of force from the kinetics analysis (Figure 2) as well as that obtained from the equilibrium analysis (see the Supporting Information). Physically this means that the DNA requires no additional elongation in order to allow the ligand to unthread. These elongation values differ significantly from those for Δ,Δ-**P**, where $\Delta x_{eq} = 0.19 \pm 0.01$ nm, with $x_{on} = 0.33 \pm 0.01$ nm and $x_{off} = 0.14 \pm 0.01$ nm.[30] Δ,Δ-**P** requires not only larger DNA elongations to thread but also significant elongation to unthread from the duplex. These results confirm the conclusion that the sterically smaller Δ,Δ-**B** deforms the DNA significantly less than the larger Δ,Δ-**P**. To better visualize the differences in binding between the two ligands, the free energy landscape was approximated for both ligands (Figure 3). The smaller DNA elongation required for Δ,Δ-**B** to bind results in a smaller free energy barrier for binding and thus faster association kinetics, while the extra elongation for unthreading required by Δ,Δ-**P** results in a molecular lock mechanism. That is, the length change needed to unthread from the DNA serves to lock the bound Δ,Δ-**P** ligands into the DNA, decreasing the dissociation rate. For Δ,Δ-**B** there is no step requiring elongation that limits the DNA unthreading rate, which accounts for the faster dissociation kinetics from DNA compared with Δ,Δ-**P**. However, these properties ($x_{on} = 0.26 \pm 0.01$ nm and $x_{off} = -0.02 \pm 0.01$ nm for Δ,Δ-**B**) contrast strongly with those of conventional intercalators such as YO, for which $x_{on} = 0.03 \pm 0.05$ nm and $x_{off} = -0.28 \pm 0.04$ nm.[38] This suggests that for association by Δ,Δ-**B** (and also by Δ,Δ-**P**), the rate-limiting step requires a significant DNA length change, which is not the case for YO. This result is consistent with the idea that base-pair opening is the rate-limiting step for threading intercalation, while DNA base pair unstacking, though required, is not the rate-limiting step for conventional intercalation.

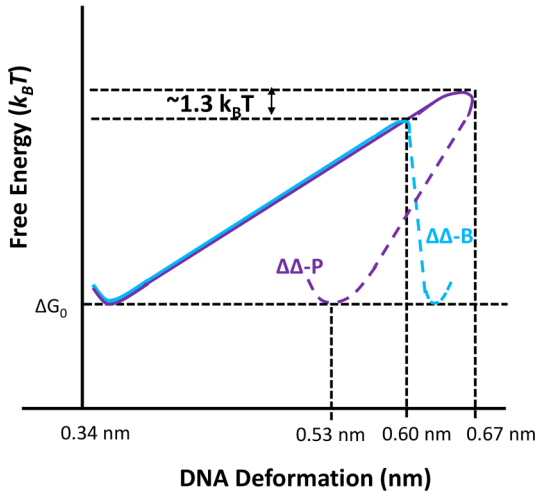

Figure 3. Comparison of the free energy landscape for binding of Δ,Δ-**B** to DNA (blue) with the free energy landscape for binding of its parent molecule Δ,Δ-**P** (violet). The solid lines represents the energy changes while lengthening toward insertion of the ligand, and the dashed lines represent relaxation back to the equilibrium lengthening. The dashed blue line indicates that Δ,Δ-**B** shows no lock mechanism, unlike the parent molecule.

In this work, the effects of steric bulk on the kinetics and mechanism of DNA threading intercalation were isolated from the equilibrium DNA binding interactions using single-molecule force spectroscopy. The DNA−ligand binding kinetics measurements revealed the significantly faster binding and unbinding of the smaller molecule, while also showing that the two molecules have similar binding affinities. These measurements provided complementary determinations of the less extreme DNA deformations needed for a sterically smaller molecule (Δ,Δ-**B**) to bind to and dissociate from the DNA relative to Δ,Δ-**P**. Thus, the steric bulk of the threading moiety is responsible for modulating the binding kinetics as well as affecting the deformation of the duplex needed for this important intercalation mechanism.

ASSOCIATED CONTENT

Supporting Information

The Supporting Information is available free of charge on the ACS Publications website at DOI: 10.1021/acs.biochem.7b01036.

Data analysis methodology, kinetics and equilibrium measurement and analysis methods, and approximate free energy landscape (PDF)

AUTHOR INFORMATION

Corresponding Authors

*E-mail: thaya@bridgew.edu.

*E-mail: mark@neu.edu.

DOI: 10.1021/acs.biochem.7b01036
Biochemistry 2018, 57, 614−619

ORCID

Fredrik Westerlund: 0000-0002-4767-4868
Mark C. Williams: 0000-0003-3219-376X

Funding

This work was funded by NSF Grant MCB-1243883 to M.C.W. A.G.C. was funded by a Northeastern University Lawrence Research Fellowship, a Physics Research Co-op Award, and an Altshuler Research Fellowship.

Notes

The authors declare no competing financial interest.

REFERENCES

(1) Muller, W., and Crothers, D. M. (1968) Studies of the binding of actinomycin and related compounds to DNA. *J. Mol. Biol. 35*, 251−290.

(2) Hurley, L. H. (2002) DNA and its associated processes as targets for cancer therapy. *Nat. Rev. Cancer 2*, 188−200.

(3) Chaurasiya, K. R., Paramanathan, T., McCauley, M. J., and Williams, M. C. (2010) Biophysical characterization of DNA binding from single molecule force measurements. *Phys. Life Rev. 7*, 299−341.

(4) Johnson, N. P., Mazard, A. M., Escalier, J., and Macquet, J. P. (1985) Mechanism of the Reaction between Cis-$[PtCl_2(NH_3)_2]$ and DNA in Vitro. *J. Am. Chem. Soc. 107*, 6376−6380.

(5) Kopka, M. L., Yoon, C., Goodsell, D., Pjura, P., and Dickerson, R. E. (1985) Binding of an antitumor drug to DNA, Netropsin and C-G-C-G-A-A-T-T-BrC-G-C-G. *J. Mol. Biol. 183*, 553−563.

(6) Goodsell, D., and Dickerson, R. E. (1986) Isohelical Analysis of DNA Groove-Binding Drugs. *J. Med. Chem. 29*, 727−733.

(7) Alderden, R. A., Mellor, H. R., Modok, S., Hambley, T. W., and Callaghan, R. (2006) Cytotoxic efficacy of an anthraquinone linked platinum anticancer drug. *Biochem. Pharmacol. 71*, 1136−1145.

(8) Paramanathan, T., Vladescu, I., McCauley, M. J., Rouzina, I., and Williams, M. C. (2012) Force spectroscopy reveals the DNA structural dynamics that govern the slow binding of Actinomycin D. *Nucleic Acids Res. 40*, 4925−4932.

(9) Yasbin, R. E., Matthews, C. R., and Clarke, M. J. (1980) Mutagenic and toxic effects of ruthenium. *Chem.-Biol. Interact. 31*, 355−365.

(10) Jiang, G. B., Xie, Y. Y., Lin, G. J., Huang, H. L., Liang, Z. H., and Liu, Y. J. (2013) Synthesis, characterization, DNA interaction, antioxidant and anticancer activity studies of ruthenium(II) polypyridyl complexes. *J. Photochem. Photobiol., B 129*, 48−56.

(11) Clarke, M. J., Zhu, F., and Frasca, D. R. (1999) Non-platinum chemotherapeutic metallopharmaceuticals. *Chem. Rev. 99*, 2511−2534.

(12) Allardyce, C. S., and Dyson, P. J. (2001) Ruthenium in Medicine: Current Clinical Uses and Future Prospects. *Platinum Met. Rev. 45*, 62−69.

(13) Rademaker-Lakhai, J. M., van den Bongard, D., Pluim, D., Beijnen, J. H., and Schellens, J. H. M. (2004) A Phase I and pharmacological study with imidazolium-*trans*-DMSO-imidazole-tetrachlororuthenate, a novel ruthenium anticancer agent. *Clin. Cancer Res. 10*, 3717−3727.

(14) Bergamo, A., Masi, A., Jakupec, M. A., Keppler, B. K., and Sava, G. (2009) Inhibitory Effects of the Ruthenium Complex KP1019 in Models of Mammary Cancer Cell Migration and Invasion. *Met.-Based Drugs 2009*, 681270.

(15) Barton, J. K., Danishefsky, A. T., and Goldberg, J. M. (1984) Tris(Phenanthroline)Ruthenium(II) - Stereoselectivity in Binding to DNA. *J. Am. Chem. Soc. 106*, 2172−2176.

(16) Lincoln, P., and Norden, B. (1996) Binuclear ruthenium(II) phenanthroline compounds with extreme binding affinity for DNA. *Chem. Commun.*, 2145−2146.

(17) Onfelt, B., Lincoln, P., and Norden, B. (2001) Enantioselective DNA threading dynamics by phenazine-linked $[Ru(phen)_2dppz]^{2+}$ dimers. *J. Am. Chem. Soc. 123*, 3630−3637.

(18) Wilhelmsson, L. M., Westerlund, F., Lincoln, P., and Norden, B. (2002) DNA-binding of semirigid binuclear ruthenium complex delta,delta-[mu-(11,11′-bidppz)(phen)(4)ru(2)](4+): extremely slow intercalation kinetics. *J. Am. Chem. Soc. 124*, 12092−12093.

(19) Westerlund, F., Eng, M. P., Winters, M. U., and Lincoln, P. (2007) Binding geometry and photophysical properties of DNA-threading binuclear ruthenium complexes. *J. Phys. Chem. B 111*, 310−317.

(20) Westerlund, F., Nordell, P., Norden, B., and Lincoln, P. (2007) Kinetic characterization of an extremely slow DNA binding equilibrium. *J. Phys. Chem. B 111*, 9132−9137.

(21) Almaqwashi, A. A., Paramanathan, T., Rouzina, I., and Williams, M. C. (2016) Mechanisms of small molecule-DNA interactions probed by single-molecule force spectroscopy. *Nucleic Acids Res. 44*, 3971−3988.

(22) Arora, S. K. (1983) Molecular-Structure, Absolute Stereochemistry, and Interactions of Nogalamycin, a DNA-Binding Anthracycline Anti-Tumor Antibiotic. *J. Am. Chem. Soc. 105*, 1328−1332.

(23) Bahira, M., McCauley, M. J., Almaqwashi, A. A., Lincoln, P., Westerlund, F., Rouzina, I., and Williams, M. C. (2015) A ruthenium dimer complex with a flexible linker slowly threads between DNA bases in two distinct steps. *Nucleic Acids Res. 43*, 8856−8867.

(24) Westerlund, F., Nordell, P., Blechinger, J., Santos, T. M., Norden, B., and Lincoln, P. (2008) Complex DNA binding kinetics resolved by combined circular dichroism and luminescence analysis. *J. Phys. Chem. B 112*, 6688−6694.

(25) Andersson, J., Fornander, L. H., Abrahamsson, M., Tuite, E., Nordell, P., and Lincoln, P. (2013) Lifetime heterogeneity of DNA-bound dppz complexes originates from distinct intercalation geometries determined by complex-complex interactions. *Inorg. Chem. 52*, 1151−1159.

(26) Andersson, J., Li, M., and Lincoln, P. (2010) AT-specific DNA binding of binuclear ruthenium complexes at the border of threading intercalation. *Chem. - Eur. J. 16*, 11037−11046.

(27) Almaqwashi, A. A., Andersson, J., Lincoln, P., Rouzina, I., Westerlund, F., and Williams, M. C. (2016) Dissecting the Dynamic Pathways of Stereoselective DNA Threading Intercalation. *Biophys. J. 110*, 1255−1263.

(28) Vladescu, I. D., McCauley, M. J., Nunez, M. E., Rouzina, I., and Williams, M. C. (2007) Quantifying force-dependent and zero-force DNA intercalation by single-molecule stretching. *Nat. Methods 4*, 517−522.

(29) Mihailovic, A., Vladescu, I., McCauley, M., Ly, E., Williams, M. C., Spain, E. M., and Nunez, M. E. (2006) Exploring the interaction of ruthenium(II) polypyridyl complexes with DNA using single-molecule techniques. *Langmuir 22*, 4699−4709.

(30) Almaqwashi, A. A., Paramanathan, T., Lincoln, P., Rouzina, I., Westerlund, F., and Williams, M. C. (2014) Strong DNA deformation required for extremely slow DNA threading intercalation by a binuclear ruthenium complex. *Nucleic Acids Res. 42*, 11634−11641.

(31) Wilhelmsson, L. M., Esbjorner, E. K., Westerlund, F., Norden, B., and Lincoln, P. (2003)) Meso stereoisomer as a probe of enantioselective threading intercalation of semirigid ruthenium complex $[\mu\text{-}(11,11'\text{-bidppz})(phen)_4Ru_2]^{4+}$. *J. Phys. Chem. B 107*, 11784−11793.

(32) Paramanathan, T., Westerlund, F., McCauley, M. J., Rouzina, I., Lincoln, P., and Williams, M. C. (2008) Mechanically manipulating the DNA threading intercalation rate. *J. Am. Chem. Soc. 130*, 3752−3753.

(33) Boer, D. R., Wu, L. S., Lincoln, P., and Coll, M. (2014) Thread Insertion of a Bis(dipyridophenazine) Diruthenium Complex into the DNA Double Helix by the Extrusion of AT Base Pairs and Cross-Linking of DNA Duplexes. *Angew. Chem., Int. Ed. 53*, 1949−1952.

(34) Niyazi, H., Hall, J. P., O'Sullivan, K., Winter, G., Sorensen, T., Kelly, J. M., and Cardin, C. J. (2012) Crystal structures of Lambda-[Ru(phen)(2)dppz](2+) with oligonucleotides containing TA/TA and AT/AT steps show two intercalation modes. *Nat. Chem. 4*, 621−628.

(35) Song, H., Kaiser, J. T., and Barton, J. K. (2012) Crystal structure of Delta-[Ru(bpy)(2)dppz](2+) bound to mismatched DNA reveals

DOI: 10.1021/acs.biochem.7b01036
Biochemistry 2018, 57, 614−619

side-by-side metalloinsertion and intercalation. *Nat. Chem. 4*, 615−620.
(36) Nordell, P., Westerlund, F., Wilhelmsson, L. M., Norden, B., and Lincoln, P. (2007) Kinetic recognition of AT-rich DNA by ruthenium complexes. *Angew. Chem., Int. Ed. 46*, 2203−2206.
(37) Almaqwashi, A. A., Andersson, J., Lincoln, P., Rouzina, I., Westerlund, F., and Williams, M. C. (2016) DNA intercalation optimized by two-step molecular lock mechanism. *Sci. Rep. 6*, 37993.
(38) Biebricher, A. S., Heller, I., Roijmans, R. F., Hoekstra, T. P., Peterman, E. J., and Wuite, G. J. (2015) The impact of DNA intercalators on DNA and DNA-processing enzymes elucidated through force-dependent binding kinetics. *Nat. Commun. 6*, 7304.

DOI: 10.1021/acs.biochem.7b01036
Biochemistry 2018, 57, 614−619